NASA CR-144708

STUDY OF THE ABLATIVE EFFECTS ON TEKTITE

Prepared by

AVCO SYSTEMS DIVISION
201 Lowell Street
Wilmington, Massachusetts 01887

Final Report, Contract NAS5-20541
AVSD-0249-75-CR

June, 1975

By

Karl K. Chen

Prepared for

NATIONAL AERONAUTICS AND SPACE ADMINISTRATION
GODDARD SPACE FLIGHT CENTER
Greenbelt Road
Greenbelt, Maryland 20771

PREFACE

The tumbling and surface roughness effects on the trajectory of entry tektite are studied in both free molecular and continuum flows. It was concluded that, while surface roughness has negligible effect on trajectory, the tumbling may play an important role in tektite trajectory and the consequent ablation, provided the body shape is different from a sphere. A shape factor B was proposed to measure the shape irregularity and was found to be a good parameter for correlations between body shape and tumbling effects.

Table of Contents

Nomenclature

A	area
a	deceleration
a_e	thermal accommodation coefficient
A	reference cross-sectional area
B	shape factor
C_D	drag coefficient
C_f	skin friction coefficient
D	diameter of equivalent sphere
d	cylinder diameter
F_A	axial drag force
F_D	total drag force
F_T	transverse drag force
$\vec{i}$	coordinate vector in Fig. 1
$\vec{j}$	coordinate vector in Fig. 1
$\vec{k}$	coordinate vector in Fig. 1
K	roughness height
K_n	Knudsen number
$\vec{l}$	unit vector along cylinder axis
l	clinder length
L	length scale
M	Mach number
P	pressure
q	dynamic pressure
R_e	Reynolds number
R_N	nose radius

Nomenclature (Cont'd)

S	total surface area
T	temperature or total time
t	time
V	velocity
V_P	total volume
W	weight
α	angle of attack
β	ballistic coefficient
γ	flight path angle
Δ	shock stand-off distance
δ	boundary layer thickness
ϵ	density ratio across the shock
ζ	speed ratio
θ	angle between V and W (Fig. 1)
ϕ	azimuth angle of cylinder axis; or angle between surface normal and velocity
λ	mean free path
μ	viscosity
ρ	density
ω	angular velocity

Subscripts

A	axial
C	continuum
e	entry condition, or edge of boundary layer
ed	end-on position
FM	free molecular flow
Λ	roughness
s	stagnation, or side wall
sd	side-on position
sp	equivalent sphere
sm	smooth
T	transverse
w	wall
z	conditions behind shock
∞	free stream

INTRODUCTION

Most works of tektite ablation studies[1, 2] were under the assumption that the entry tektite is of spherical shape and smooth surface. The numerical results of those calculations indicated that ablation takes place mainly by melt flow rather than by vaporization.[1-2] This is disturbing in comparison with the observations on the recovered tektite, since melt flow has not been definitely found on tektite except for autstrlite and a few javanites. The effects of surface roughness on boundary layer transition, heating and ablation have been studied in Reference 3, which concluded that the surface roughness on most recovered tektite was formed before earth entry. Consequently, the roughness may trip the boundary layers to turbulence and enhance vaporization. Numerical results in Reference 3 indicated that the effect of surface roughness on ablation appeared to be an important factor to explain the discrepancy of vaporization vs melt flow. The effect of surface roughness on drag has not been discussed in Reference 3.

Most of the entry tektites are expected to be nonspherical in shape and to carry a not negligible rotational momentum. In addition, irregular or asymmetrical bodies, in which the resultant of aerodynamic pressure doesn't pass through the center of mass, will experience the action of a variable couple influencing rotation. Thus, one way or the other, the entry tektite is expected to be tumbling in some fashion. Since the drag coefficient is highly dependent on the angle of attack, the effective ballistic coefficient (or the trajectory) and the total ablation may be substantially different from the value of correspoinding spherical bodies. In this paper, analysis were conducted under the assumption that the frequency of tumble is large compared to the change in altitude during any cycle; thus, the average drag coefficient may be associated with the fixed environment of a single altitude. The correction of drag coefficient will change the trajectory of entry tektite, affecting the corresponding albation behavior.

During earth entry, tektite experienced various regions of atmosphere, from free molecular flow, transition flow to continuum flow, depending on the corresponding density level. The division of gas dynamics into various regions are usually conducted based on characteristic reanges of values of an appropriate Knudson number, defined by a dimensionless ratio λ/L, where λ denotes molecular mean free path and L is a length scale. There are various ways in defining λ and L; e.g. the mean free path may be measured at freestream or behind the shock, while the length scale L may be referred to as the nose radius R_N, boundary layer thickness δ, or the shock stand off distance Δ, depending on the parameters and the environments.

Flow in the various transition regimes between free-molecular and continuum is extremely complicated, and no satisfactory theoretical solution has yet been offered. No detailed development of drag coefficients or skin friction will be presented in this report for transitional flows. Discussions will be concentrated on the limits of free-molecular and continuum flows. Engineering methods will be presented for extrapolating drag coefficients and skin frictions between these two well defined regimes.

In free molecular region, the mean free path is everywhere very much greater than a characteristic body dimension, and the distortion of the free stream velocity distribution due to the presence of the body is negligible. However, the actual transfer processes are tied up with the fact that the molecules are remitted or reflected in some manner; thus, a thermal accommodation coefficient is introduced to measure the extent to which the mean energy of the remitted molecules is accommodated toward an energy corresponding to the temperature of the wall. The thermal accommodation coefficient is defined by the equation

$$a_e = \frac{E_i - E_r}{E_i - E_b} \qquad (1)$$

where E_i is the incident energy per unit surface area per second, E_r is the reflected or re-emitted energy carried away by the molecules as they leave the body, and E_b is the energy that the re-emitted or reflected stream would have if all the incident molecules were re-emitted with a Maxwellian velocity distributions corresponding to the surface temperature T_w. Tests of Wiedmann and Trumpler[4] indicate that under static conditions, the thermal accommodation coefficient for air on various typical engineering surfaces lies between 0.87 and 0.97. Thus, it is reasonable to use unity accommodation coefficient for most practical problems.

The other important parameter in rarefied gases is the so called speed ratio, ζ, which is defined as the ratio of the mass velocity to the most probable random speed in the freestream. It was estimated in Reference (5) that the average of air molecules at high altitudes to be about 4000-5000 ft./sec.: an order of magnitude less than the typical speed of tektite entry. Under the assumption of unity accommodation coefficient that the air molecules are reflected at roughly the same temperature as the tektite, the reflected particle should have velocities at the neighborhood of 3000 to 4000 ft./sec. Since the molecular velocity before and after the collision with tektite is much less than tektite velocity, the molecular velocity incident to tektite can be approximated by the tektite velocity itself and the rebouncing velocity of air molecules can be approximated by zero. Thus, the approximation of infinite speed ratio, ζ, will be used throughout the analysis of free molecular flow.

The other limit of the flow regimes is the well-studied continuum flows at sufficiently high Reynolds numbers. The viscous effects in this region may be taken into account using classical boundary layer theory, with suitable modification for pressure interaction if appropriate. Pressure drags on bodies traveling with hypersonic speed can be estimated with Newtonian approximation, while surface roughness effects can be calculated from classic boundary layer theory. With the free molecular and continuum flow results calculated, the quantities in transitional flows can be interpolated between these two well defined regions.

Tektite analysis contain a source of error depending on the various shape of the tektite, except when the latter is nearly spherical such as australite. However, australite composed only a small portion of the recovered tektite, and indeed most of the tektite are irregular in shape and do not lend themselves to purely analytical analysis. Certain plausible assumptions can be made in this respect for order of magnitude calculations. To measure the geometry of an entering tektite, a shape factor B(6) is defined as the actual surface area divided by the surface area of a sphere of equivalent volume,

$$B = S/\pi D^2 \tag{2}$$

where S is the tektite surface area and D is the diameter of the equivalent sphere,

$$D = (6 V_p/\pi)^{1/3} \tag{3}$$

with V_p denoting the volume of tektite.

Parametric studies for tektite shape effects on trajectory and ablation will be carried out in terms of shape factor B with circular cylinder used as basic shape for numerical results. It is hoped that simple analysis can bring out the order of magnitude effect of body shape on tektite entry behavior.

The surface area and volume of a circular cylinder of diameter d and length ℓ are respectively as follows:

$$\begin{aligned} S &= \pi/2\ d^2 + \pi\ d\ell \\ V_p &= \pi/4\ \ d\ell \end{aligned} \tag{4}$$

Substitution of Eq. (4) into (2) and (3) yields the diameter of equivalent sphere D and the shape factor B,

$$\begin{aligned} D &= 1.1447\ d^{2/3}\ \ \ell^{1/3} \\ B &= 0.3816\ (d/\ell)^{2/3} + 0.7631\ (\ell/d)^{1/3} \end{aligned} \tag{5}$$

Dependence of B on d/ℓ is plotted in Figure 1. It is indicated that B tends to increase in both long cylinder ($\ell/d > 1$) and short cylinder ($\ell/d < 1$) with a minimum at $\ell = d$. Both long cylinder and short cylinder results will be presented in this report, and the inference of these results to tektite study will depend on the actual shape of tektite.

TUMBLING AT FREE MOLECULAR FLOWS

The trajectory of a body entering the atmosphere from high altitude depends greatly on the entry velocity Ve, the entry flight path angle γ_e and the ballistic coefficient β which is defined as

$$\beta = W/C_D A \tag{6}$$

where W is the weight of the body, and C_D and A are the drag coefficient and the corresponding reference area respectively. While Ve and γ_e specify the initial conditions of earth entry, the ballistic coefficient is a function of Mach number, Reynolds number, and geometry of the entry object. Thus, the key factor for trajectory calculation is the determination of β.

Under the approximations of unity accommodation coefficient A_e and infinite speed ratio s, the drag on tektite at free molecular flow is actually equal to the change in momentum of all the air molecules striking the surface per unit time; i.e.

$$F_D = \rho_\infty V_\infty^2 A \tag{7}$$

where ρ_∞, V_∞ and A denote the corresponding atmosphere density, tektite velocity and projected front area respectively. Thus, C_D for free molecular flow can be well approximated by 2, based on the projected front area. This leads to the following expressions of ballistic coefficient

$$\beta_{sd} = W/(2 \ell d) \tag{8}$$

for cylinder at side-on positition (cylinder axis $\perp$ flow)

$$\beta_{ed} = 2W/\pi d^2 \tag{9}$$

for cylinder at end-on position (cylinder axis $\parallel$ flow) and

$$\beta_{sp} = W/(2.0583\ d^{4/3}\ \ell^{2/3}) \tag{10}$$

for equivalent sphere, where W denotes weight, and ℓ and d are the length and the diameter of the cylinder respectively.

The same argument leads to the corresponding ballistic coefficient

$$\beta = W/(2d\ell \sin\alpha + \pi/2\ d^2 \cos\alpha) \tag{11}$$

For a tumbling body, the average ballistic coefficient is defined as being $W/C_D A$ of an object which has the same deceleration

as the average decelerations:

$$\bar{a} \equiv 1/T \int_0^T a(t)\, dt \tag{12}$$

where a and t denote deceleration and time respectively, and q_∞ is the dynamic pressure which is assumed not vary greatly during T. By definition of average $W/C_D A$

$$\bar{a} = q_\infty / \bar{\beta} \tag{13}$$

and, therefore,

$$\bar{\beta} = \left[\frac{1}{T} \int_0^T \frac{dt}{\beta(t)} \right]^{-1} \tag{14}$$

If the motion of a cylinder is assumed tumbling in the trajectory plane (i.e. $\vec{\omega} \cdot \vec{V} = 0$) and the variation of angular velocity ω is small during T, thus,

$$\alpha = wt \tag{15}$$

and the average ballistic coefficient in terms of α is given by,

$$\bar{\beta} = \left[\frac{2}{\pi} \int_0^{\pi/2} \frac{d\alpha}{\beta(\alpha)} \right]^{-1} \tag{16}$$

substitution of Eq. (11) into eq. (16) yields

$$\bar{\beta} = W/(4/\pi \ell d + d^2) \tag{17}$$

However, since tektites are probably put out at random spin orientation, it will in general be true that

$$\vec{\omega} \cdot \vec{V} \neq 0 \tag{18}$$

so that the actual $\bar{\beta}$ will be different from that given by eq. (17).

Figure 2 shows a $(\vec{i}, \vec{j}, \vec{k})$ coordinate system with velocity vector in the $\vec{k}$ direction, the $\vec{\omega}$ vector at an angle θ with the velocity vector and in the $\vec{k} - \vec{j}$ plane. The angle α is the angle between the cylinder axis and the velocity vector $\vec{V}$, and the angle $\phi = \omega t$ is the azimuth angle of the cylinder axis, $\vec{\ell}$. From Figure 2 it is obvious that

$$\frac{\vec{\omega}}{\omega} = \vec{k} \cos\theta + \vec{j} \sin\theta \tag{19}$$

$$\vec{\ell} = \left(\vec{\iota} \times \frac{\vec{\omega}}{\omega}\right) \cos \phi + \vec{\iota} \sin \phi \qquad (20)$$

$$\cos \alpha = \vec{k} \cdot \vec{\ell} = \sin \theta \sin \phi \qquad (21)$$

Substituting (21) into (11), and (16) we obtain the approximate solution

$$\bar{\beta}\ (\theta) = W/\left[(2 - \tfrac{1}{2} \sin^2\theta - 3/32 \sin^4\theta)\, \ell d + d^2 \sin\theta\right] \qquad (22)$$

where a slight adjustment has been made to some of the sine terms to allow $\beta(\pi/2)$ matching eq. (17). Thus, at each value of $\theta = \theta_o$, $(0 \leq \theta \leq \pi/2)$ an effect ballistic coefficient $\beta(\theta_o)$ can be determined which represents the average taken over a cycle of tumbling in the plane defined by θ_o. As indicated earlier, no attempt is made to predict specific orientation of the plane of tumble in the present paper. Instead, an average value of the effective ballistic coefficient is defined for a random orientation of the plane of tumbling by the following equation.

$$\bar{\bar{\beta}} \equiv (E\ (1/\beta))^{-1} = 1 \Big/ \int_0^{\pi/2} \rho_p(\theta) \Big/ \beta(\theta)\ d\theta \qquad (23)$$

where ρ_p is the probability density. Under the assumption that ω is randomly distributed in space, it can be easily shown that the distribution function for θ is given by

$$P\ (\theta < \theta_o) = 1 - \cos \theta_o \qquad (24)$$

and the probability density is given by,

$$\rho_p(\theta) = \frac{dP}{d\theta_o}\Big|_{\theta_o = \theta} = \sin\theta \qquad (25)$$

Substitution of Eq. (25) and (22) into (23) yields,

$$\bar{\bar{\beta}} = W/(1.5166\ \ell d + 0.7854\ d^2) \qquad (26)$$

Equations (8), (9), (17) and (26) represent the ballistic coefficients of a cylinder shape at various position and tumbling patterns. Their relative values with respect to that of an equivalent sphere are summarized in Table 1. Combination of Table 1 and eq. (5) yields the numerical results plotted in Figure 3, which shows the ratio of ballistic coefficient to that of an equivalent sphere as a function of the shape factor B.

Since the shape of long cylinder differs very much from that of the corresponding short cylinder of the same shape factor B, the relative ballistic coefficient of an irregularly shaped tektite is expected to be somewhere between or close to those of the long and short cylinders. Both results of tumbling in pitch plane and of random tumbling are included in Figure 3 to cover the range of various styles of tumbling. Thus, once the volume and the surface

area of a tektite shape are measured, the range of ballistic coefficient can be estimated from the cross-hatched area in Figure 3. Since the shape of tektite can have a shape factor B of 2~3, the drag acting on it can easily be 2~3 times larger than that of the equivalent sphere.

TUMBLING IN CONTINUUM AND TRANSITIONAL FLOWS

As the tektite approaching continuum flow region, the mean free path becomes negligibly small compared to the dimension of tektite and the viscous effects are limited to a thin layer over the body surface (boundary layer). Because of the hypersonic speed, a modified Newtonian pressure distribution appears to be appropriate for mcse practical problems. The local pressure is given by

$$P = P_{\infty} + (P_s - P_{\infty}) \cos^2 \phi \qquad (27)$$

where P is pressure, ϕ is the angle between the surface normal and the velocity and subscripts ∞ and s denote the conditions at free-stream and at stagnation point respectively. The continuity and momentum equations across a normal shock are

$$\rho_{\infty} V_{\infty} = \rho_2 V_2$$

$$P_{\infty} + \rho_{\infty} V_{\infty}^2 = P_2 + \rho_2 V_2^2$$

where ρ and V are density and velocity respectively, and subscript 2 denotes condition immediately after the normal shock. Since incompressible flow relations closely approximate actual conditions in the stagnation region behind the shock wave, the stagnation pressure can be given by

$$P_s = P_2 + \tfrac{1}{2} \rho_2 V_2^2$$

Thus, eq. (27) becomes

$$P = P_{\infty} + q_{\infty} (2 - \rho_{\infty} / \rho_2) \cos^2 \phi$$

For Mach number greater than 10, $P_{\infty} \ll q_{\infty}$ and $P_s \simeq q_{\infty} (2 - \rho_{\infty}/\rho_2)$ and the following simplified relations have been frequently used for practical purpose:

$$P \simeq q_{\infty} (2 - \epsilon) \cos^2 \phi \simeq P_s \cos^2 \phi \qquad (28)$$

where ϵ denotes ρ_{∞} / ρ_2.

The drag coefficient is given by

$$C_D = \int P \cos \phi \, dA / q_{\infty} A_r \qquad (29)$$

which is integrated over the surface of the body exposed to the freestream. For the case of a cylinder in side-on position, Eq. (29) yields

$$C_D = 2/3\ (2 - \epsilon) \tag{30}$$

which lead the side-on ballistic coefficient

$$\beta_{sd} = W/\left[2/3\ \ell d\ (2 - \epsilon)\right] \tag{31}$$

In addition, Eq. (29) leads to the drag coefficient and ballistic coefficient of the equivalent sphere as follows:

$$C_D = 1/2\ (2 - \epsilon)$$
$$\beta_{sp} = W/\left[0.5146\ (2 - \epsilon)\ d^{4/3}\ \ell^{2/3}\right] \tag{32}$$

As to the end-on position, there would be a uniform pressure P_s over the face of the cylinder according to Newtonian theory. However, Stoney and Swanson(7) found that the average pressure on the face of a cylinder 0.909 times stagnation pressure. Using this value in Eq. (29) and integrating, we have, for a cylinder in end-on position,

$$C_D = 0.909\ (2 - \epsilon)$$
$$\beta_{ed} = W/\left[0.714\ (2 - \epsilon)\ d^2\right] \tag{33}$$

For a cylinder at angle of attack, the total drag force can be approximated by the vector sum of the axial and transverse components

$$F_D = F_T \sin\alpha + F_A \cos\alpha$$

or

$$C_{D\alpha}\ q_\infty\ A_\ell = C_{D_T}\ q_T\ A_\ell\ \sin\alpha + C_{DA}\ q_A\ A_\ell \cos\alpha \tag{34}$$

but

$$q_T = \tfrac{1}{2}\rho_\infty\ V_T^2 = q_\infty\ \sin^2\alpha \tag{35}$$

and

$$q_A = \tfrac{1}{2}\rho_\infty\ V_A^2 = q_\infty\ \cos^2\alpha \tag{36}$$

Combination of eqs. (34), (35), (36), and the definition of ballistic coefficient yields,

$$\beta(\alpha) = W/\left[(2/3\ \sin\alpha\ \ell d + 0.714\ \cos^3\alpha\ d)\ (2 - \epsilon)\right] \tag{37}$$

The average ballistic coefficient for a cylinder tumbling in the trajectory plane is given by substituting Eq. (38) into (16),

$$\bar{\beta} = W/\left[(0.2829\,\ell d + 0.3030\,d^2)\,(2-\epsilon)\right] \qquad (38)$$

For cylinder tumbling in plane at an angle $(\pi/2 - \theta)$ with the trajectory plane, the average ballistic coefficient can be calculated by the substitution of Eqs. (21) and (38) into (16). An approximate solution was obtained,

$$\bar{\beta}(\theta) = W/\left[(0.6667 - 048\sin^2\theta + 0.1\sin^4\theta + 0.303\,\frac{d}{\ell}\sin^3\theta)(2-\epsilon)\,\ell d\right] \qquad (39)$$

where a slight adjustment has been made to some of the sine terms to allow $\bar{\beta}(\pi/2)$ matching Eq. (38). The average ballistic coefficient of a cylinder tumbling in random is given by substitution of Eq. (39) into (23),

$$\bar{\bar{\beta}} = W/\left[(0.4\,\ell d + 0.1785\,d^2)\,(2-\epsilon)\right] \qquad (40)$$

Table 1 summarizes the relative ballistic coefficients of a cylinder traveling in continuum flow at various positions and tumbling patterns. Combination of Table 1 and Eq. (5) yields the variation of those relative ballistic coefficients against shape factor B as plotted in Figure 4.

As for drag coefficient in transition regions between free molecular and continuum flows, Bloxson and Rhodes[8] conducted a series of drag coefficient experiments in a hypersonic wind tunnel on bodies of various shapes with Knudsen number range 0.0001 - 0.34. The Knudsen number there was defined as 1/3 mean free path behind shock divided by the shock stand-off distance, i.e.

$$K_n = \lambda/3\Delta \qquad (41)$$

The drag coefficients so obtained on spheres are plotted in Figure 5 as a function of Knudsen number, which shows that drag coefficients can be presented as an exponential function of Knudsen number in transition flow.

The most remarkable point about Figure 5 is that all of the shapes considered have the same C_D variation with K_n in the transition region and the same drag coefficient in the free molecular region. The variation seems to hold for any shape and gas, having only the requirement that the flow is over Mach number 4. An empirical formula was derived based on the data of spherical bodies in Reference 8; i.e.

$$C_D = \frac{C_{D,C} + C_{D,FM}}{2} + \left(\frac{C_{D,C} - C_{D,FM}}{2}\right)\frac{K_n^{1.52} - 0.0504}{K_n^{1.52} + 0.0504} \qquad (42)$$

where $C_{D,\,FM}$ and $C_{D,\,C}$ denote the drag coefficients in free-molecular and continuum regions respectively.

ROUGHNESS EFFECT

Surface roughness is known to promote laminar-turbulent transition and to increase surface drag and heating by a significant amount. The surface drag on rough surfaces depends on the number of roughness elements per unit area, on their shapes and heights, and on the way in which they are distributed over the surface; since the main contribution of surface drag is from the pressure force acting on the roughness elements. The number of parameters required for roughness description is extraordinarily large and no analysis have been developed to include all the parameters required. Most authors measured the roughness effect on surface drag by a single parameter of effective roughness K_{eff}, defined as the roughness size of closely packed sand roughness which gives the same value of skin friction coefficient as the actual roughness.

In this way, the difficulty has been shifted to the determination of effective roughness from the measurement of actual roughness. However, for order of magnitude analysis such as tektite studies, the average height of the reasonably spaced roughness elements can be used as effective roughness for practical calculations. As discussed in Reference 3, an effective roughness, K_{eff}, equal to 40 mils is assumed for the tektite studies in this report.

The exact way to assess the surface roughness effect on trajectory is to calculate the drag coefficient of a roughened tektite which is tumbling during entry. However, the coupling phenomena of roughness and tumbling is a very complicated problem because of the cross flows involved in an inclined cylinder, which is beyond the scope of this report. The approach here is to estimate the roughness effect according to the most noticeable case, i.e., the case that roughness has maximum effect. For a long cylinder ($d/\ell < 1$), the roughness effect is maximum as the cylinder is at end-on position, and the numerical results of roughness effect will be carried out in this position.

Roughness effects on drag are closely related to the behavior of skin friction drag coefficient through various regions of earth entry. Reference 9 presented an empirical relation of the skin friction coefficients in the form of $(C_f M)$ as a function of the interaction parameter $M/\sqrt{Re}$, which is defined for flows with significant viscous effect. In such a case, the significant characteristic dimension of the flow field is the boundary layer thickness δ rather than a dimension L typical of the body itself, and the corresponding Knudson number based on the length scale δ is actually proportional to the interaction parameter $M/\sqrt{Re}$. Hoerner[9] suggested that for skin friction coefficient simple gas dynamics for continuum flows are applicable to $M/\sqrt{Re} < 10^{-2}$, and a transitional phase between 10^{-2} and 10^{+1}, above which free

molecular flow is finally established. Figure 7 presented both laminar and turbulent skin friction coefficient in terms of $C_f M$ vs $M/\sqrt{Re}$. Very good correlation is found between free molecular and continuum results. Naturally, turbulent friction should not be expected to reduce below the level as found for laminar boundary layer flows. The experimental results as plotted in Figure 6 suggest that the laminar function represents the limiting condition for the turbulent function. It appears that a low Reynolds number the distinction between laminar and turbulent boundary layer flow becomes lost. It is suggested[9] that the vorticity originating across a boundary layer induced shock wave behaves like turbulent, thus possibly rendering a "laminar" layer effectively turbulent. For surfaces containing roughness of 40 mils such as observed on many recovered tektite, the boundary layers will be tripped to turbulence somewhere between $M/\sqrt{Re} \simeq 10^{-1}$ and 1 according to the numerical results in Reference 3; and turbulence exists in boundary layers in most of the transitional region. Thus, it is plausible to use the conventional analysis of roughness effect in turbulent flow through the whole trajectory of tektite entry.

The effect of roughness on turbulent skin friction has received considerable investigation in low speed flow as summarized by Clauser.[10] The roughness skin friction in high speed flow was studied by Goddard,[11] who showed that the effect of compressiblility can count as a reduction in wall density as Mach number increased. In addition, the skin friction increase due to roughness correlated with the roughness Reynolds number $Re_K^* \equiv \rho_w u_\tau K/\mu_w$ independent of Mach number. The data of Reference 11, which were limited to adiabatic flow conditions, yield a close approximation for roughness effect on skin friction:

$$(C_f/C_{fo}) = \log_{10} Re_K^* \qquad (43)$$

More recently Young[12] found that as the wall temperature was reduced, the skin friction dropped below the Goddard value for adiabatic walls. Reasoning that the effect of heat transfer was to produce a density gradient near the wall such that the effective density at the roughness surface was less than the wall value, Young developed a reference temperature method that correlated his results,

$$C_f/C_{fi} = 0.365\ (Te/Tr) + 0.635\ (Te/Tw) \qquad (44)$$

where C_{fi} is the incompressible value of C_f including roughness effect.

The relation between roughness skin friction coefficient and its adiabatic wall value can be derived directly from Eq. (44) i.e.

$$C_f/C_{f,aw} = 0.365\ (Tw/Tr) + 0.635 \qquad (45)$$

Combination of Eqs. (45) and (43) yields the relation between rough wall skin friction including heat transfer to that of smmooth wall under adiabatic conditions[13]

$$C_f/C_{f_o} = \left|0.365\ (Tw/T_\infty) + 0.635\right| \quad \log 10\ Re_K^* \qquad (46)$$

Thus, once the reynolds number around the roughness elements, the roughness size K and the temperature ratio Tw/Tr are given, the affect of surface roughness on skin friction can be calculated. The skin friction coefficient of smooth wall C_{f_o} can be estimated from the correlations in Figure 6.

The total drag for a long cylinder traveling in an end-on position can be expressed as follows:

$$F_D = q_\infty\ A_e\ \left(C_f\ \frac{q_e}{q_\infty}\ \frac{A_s}{A_e} + C_p\right) \qquad (47)$$

where C_f term denotes the friction drag acting on the sidewall of the cylinder as indicated in Figure 6 and C_p term indicates the pressure drag acting on the end face of the cylinder. Usually the friction drag for a smooth cylinder is at least three orders of magnitude less than the pressure drag, providing the area rateo A_s/A_e is of order one. This explains why only pressure drags are considered in tumbling studies. For rough surfaces, the friction drag can be larger than that of smooth wall, and its effect can be expressed by the relative drag of rough to smooth long cylinders as follows:

$$(\overline{F}_D)_{r\text{-}sm} \equiv \frac{F_{D,r}}{F_{D,sm}} = \frac{C_f\ \frac{q_e}{q_\infty}\ \frac{A_s}{A_e} + C_p}{C_{f_o}\ \frac{q_e}{q_\infty}\ \frac{A_s}{A_e} + C_p} \qquad (48)$$

where C_p can be estimated from Eqs. (9), (33), and (42) for free molecular, continuum, and transitional flows respectively, C_{f_o} from Figure 6, C_f from Eq. (46), q_e/q_∞ from hypersonic results such as in Reference 3, and A_s/A_e from geometry considerations. The area ratio A_s/A_e can be related to the shape factor B through

Eq. (5).

Figure 7 shows the relative drag of rough long cylinder to smooth one at end-on position, in which drag is presented as a function of shape factor B. The Mach number here is a constant value of 30, which is the average value in the actively ablating region of tektite entry.(3)

The Reynolds pumber here, based on the equivalent diameter of one inch, is 10^5, which is the upper limit that an entry tektite may experience according to the numerical results in Reference 3. The ratio of roughness size to the equivalent diameter, K/D, is selected to be 0.04; since the average roughness on tektite is about 40 mils and the average diameter of tektite is probably at the order of one inch. Figure 9 indicates that the drag increase due to roughness at $Re_D = 10^5$ is less than 10% for usual tektite geometry (say $1 < B < 3$). Since roughness effect on drag increases with Reynolds number, the drag increase indicated in Figure 7 gives the upper limit of roughness effect on drag for tektite entry. The Reynolds number of an entry tektite usually is much less than 10^5; thus, it is plausible to assume that the surface roughness effect on drag can be neglected for tektite entry studies.

TRAJECTORY AND ABLATION

The trajectory of a vehicle entering the atmosphere from great altitude depends greatly on the entry velocity V_e, the flight path angle γ, and the ballistic coefficient β. In general, both the flight path angle and the ballistic coefficient vary due to the presence of gravity force and to the change of drag coefficient during flight. Hence, it is clear that exact solution of the trajectory is formidable. However, in the trajectory region of active ablation, the velocity of the entry tektite is so high that its total drag is much larger than the gravity force and that the drag coefficient is nearly constant because of the corresponding high Mach number environment.[14] Thus, for a simplified trajectory analysis like this, it is appropriate to assume that both γ and β are constant. In addition, the atmosphere density ρ_∞, which is a function of altitude only, is given by the relation,

$$\rho_\infty/\rho_o = \exp\ (-\ Z/\lambda\ ) \qquad (49)$$

where ρ_o and λ are constant equal to 0.091 lbs./ft.^{3} and 23120 ft. respectively according to the curve fit for high altitude atmosphere in Figure 8. Based on these assumptions the relations, Allen and Eggers[14] derived the following relation

$$V = V_e \exp\ \left[-\rho_\infty \lambda/\ (2\ \beta \sin\gamma\ )\right] \qquad (50)$$

which can be used to estimate the vehicle velocity as a function of altitude once the parameters of the entry conditions, such as γ, β, V_e, are given.

Numerical results in Reference 3 indicate that ablation rate was practically zero if velocity reduced to or below 10,000 ft/sec. Thus, one can define a consolidating altitude at which the velocity just reaches 10,000 ft/sec and no significant ablation thereafter. Combination of Eqs. (49), (50), and (5) yields the numerical results plotted in Figure 9 which show the consolidating altitude as a function of shape factor B. The ballistic coefficient formula used in Figure 9 is based on that of random tumbling in free molecular flow with the equivalent diameter of one inch. It is clearly indicated that the shape factor B has significant effect of tumbling on trajectory. In addition, the geometry style (long or short cylinder) has only slight effect on the consolidating altitude, indicating that shape factor B is a fairly good parameter to describe irregular shapes. Figure 10 shows the similar conclusion for the trajectory calculations based on the randomly tumbling ballistic coefficient in continuum flows.

For an order of magnitude estimation, the total recession of an entry body can be measured by the total heat transfer to the body. The stagnation point heat transfer rate to a sphere of radius R_N can be approximimately calculated the following equation[N](15)

$$\dot{q}_s = 865\ R_N^{-0.5}\ (\rho_\infty/\rho_o)^{0.5}\ (V/10^4)^{3.15} \qquad (51)$$

where the unit of heat transfer rate $\dot{q}_s$ is in BTU/ft^2-sec, radius R_N in feet, and velocity V in ft/sec. Since the most obvious effect of tumbling on tektite behavior is velocity reduction due to higher drag, it is plausible to measure the ablation rate by the substitution of reduced velocity into Eq. (51). The relative total ablation of velocity reduced tektite with respect to that of equivalent sphere can be measured by the total heat transfer to the stagnation point, i.e.,

$$\frac{\Delta S_{tumb}}{\Delta S_o} \simeq \frac{\int q\ (V_{tumb})\ dt}{\int q\ (V_o)\ dt} \qquad (52)$$

where ΔS is total recession, subscript tumb and o denote tumbling correction and no tumbling respectively. Combination of Eqs. (51), (52), and (5) yields the numerical results plotted in Figure 10, where the relative total recession is presented as a function of shape factor B. The ballistic coefficient formula used in Figure 11 is based on that of random tumbling in free molecular flow with the equivalent diameter of one inch. The shape factor B has significant effect on total recession, while both γ_e and geometry style (long or short cylinder) have only negligible effects. Figure 12 shows the same conclusion for the total recession calculations based on the ballistic coefficient on continuum flow.

CONCLUSION

This study indicates that surface roughness effect on the total drag of entry tektite is negligible, and can be ignored for tektite studies. For shapes other than sphere, the tumbling of tektite has significant effect on the total drag and on the consequent entry trajectory. In addition, the shape factor B was found to be a good parameter for the measurement of irregular shape and its tumbling effect on tektite entry. Rough estimation of the tumbling effect on the total recession can be estimated once the shape factor B and the size of tektite are given.

REFERENCES

1. Chapman, D. R. and Larson, H. K., "On the Lunar Origin of Tektites," Journal of Geophysical Research, Vol. 68, No. 14, July 15, 1963, pp. 4305-4358.

2. O'Keefe III, John, A., et al., "Tektite Ablation: Some Confirming Calculations," Journal of Geophysical Research, Vol. 78, No. 17, June 10, 1973.

3. Chen, K. K., "Tektite Ablation Study," Contract NAS5-23242, AVSD-0084-74-CR, March, 1974.

4. Wiedmann, M. L., and Trumpler, P. R., "Thermal Accommodation Coefficients, Trans. A.S.M.E. 68, 57-64 (1946).

5. Klett, Robert, D., "Drag Coefficients and Heating Ratios for Right Circular Cylinders in Free Molecular and Continuum Flow from Mach 10 to 30," SC-RR-64-2171, Sandia Lab., Albuquerque, 1964.

6. Oepik, Ernst J., "Physics of Meteor Flight in the Atmosphere," Interscience Publishers, Inc., New York, 1958.

7. Stoney, W. E. and Swanson, A. G., "Heat Transfer Measured on a Flat-Face Cylinder in Free Flight at Mach Number up to 13.9," NACA RM-L-57E13, June 17, 1957.

8. Bloxson, D. E., and Rhodes, B. V., "Experimental Effect of Bluntness and Gas Rarefaction on Drag Coefficients and Stagnation Heat Transfer on Axisymmetric Shapes in Hypersonic Flow," Journal of the Aerospace Sciences, December, 1962.

9. Hoener, S. F., "Fluid-Dynamic Drag," Published by the Author, 1965.

10. Cluaser, F. H., "Turbulent Boundary Layer," Advances in Applied Mechanics, Volume IV, ed. by H. L. Dryden and T. Von Karman, Academic Press, Inc., pp. 1-21, 1956.

11. Goddard, F. E., Jr., "Effect of Uniformly Distributed Roughness on Turbulent Skin-Friction Drag at Supersonic Speeds," Journal of the Aero/Space Sciences, Volume 26, No. 1, January, 1959.

12. Young, F. L., "Experimental Investigation of the Effects of Surface Roughness on Compressible Turbulent Boundary Layer Skin Friction and Heat Transfer," University of Texas DRL 532, May 1965 (AD 621085).

REFERENCES (Concl'd)

13. Nestler, D. E., "Compressible Turbulent Boundary Layer Heat Transfer to Rough Surfaces," AIAA 3rd Fluid and Plasma Dynamics Conference, Los Angeles, Calif., June 29 - July 1, 1970.

14. Allen, H. Julian and Eggers, A. J., "A Study of the Motion and Aerodynamic Heating of Ballistic Missiles Entering the Earth Atmosphere at High Supersonic Speed," NACA Rep. 1381, 1958, pp. 1-16.

15. Detra, R. W. and Hidalgo, H., "Generalized Heat Transfer Formulas and Graphs for Nose Cone Re-entry into the Atmosphere," ARS Journal, March 1961, pp. 318-321.

TABLE 1

Relative Ballist Coefficient of a Cylinder with Respect to the Equivalent Sphere ($\beta_{sphere}/\beta_{cylinder}$)

Case	Flow Regime: Free Molecular	Flow Regime: Continuum
Side-on	$0.9717\left(\frac{\ell}{d}\right)^{1/3}$	$1.2955\left(\frac{\ell}{d}\right)^{1/3}$
End-on	$0.7632\left(\frac{d}{\ell}\right)^{2/3}$	$1.3875\left(\frac{d}{\ell}\right)^{2/3}$
Tumbling in pitch plane	$0.6186\left(\frac{\ell}{d}\right)^{1/3} + 0.4858\left(\frac{d}{\ell}\right)^{2/3}$	$0.5497\left(\frac{\ell}{d}\right)^{1/3} + 0.5888\left(\frac{d}{\ell}\right)^{2/3}$
Random tumbling	$0.7852\left(\frac{\ell}{d}\right)^{1/3} + 0.3816\left(\frac{d}{\ell}\right)^{2/3}$	$0.7773\left(\frac{\ell}{d}\right)^{1/3} + 0.3469\left(\frac{d}{\ell}\right)^{2/3}$

FIGURE I - VARIATION OF SHAPE FACTOR B FOR A CYLINDER

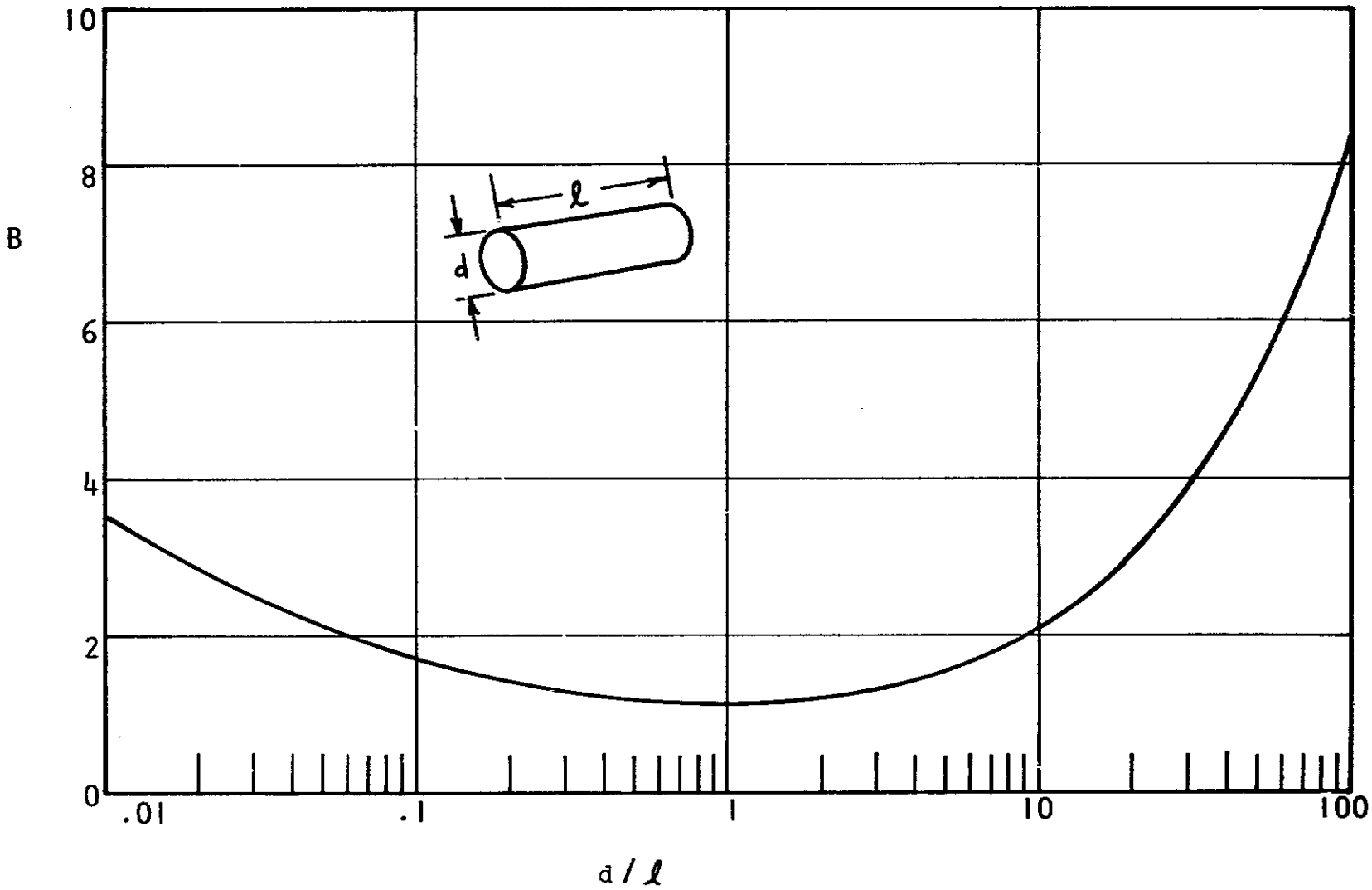

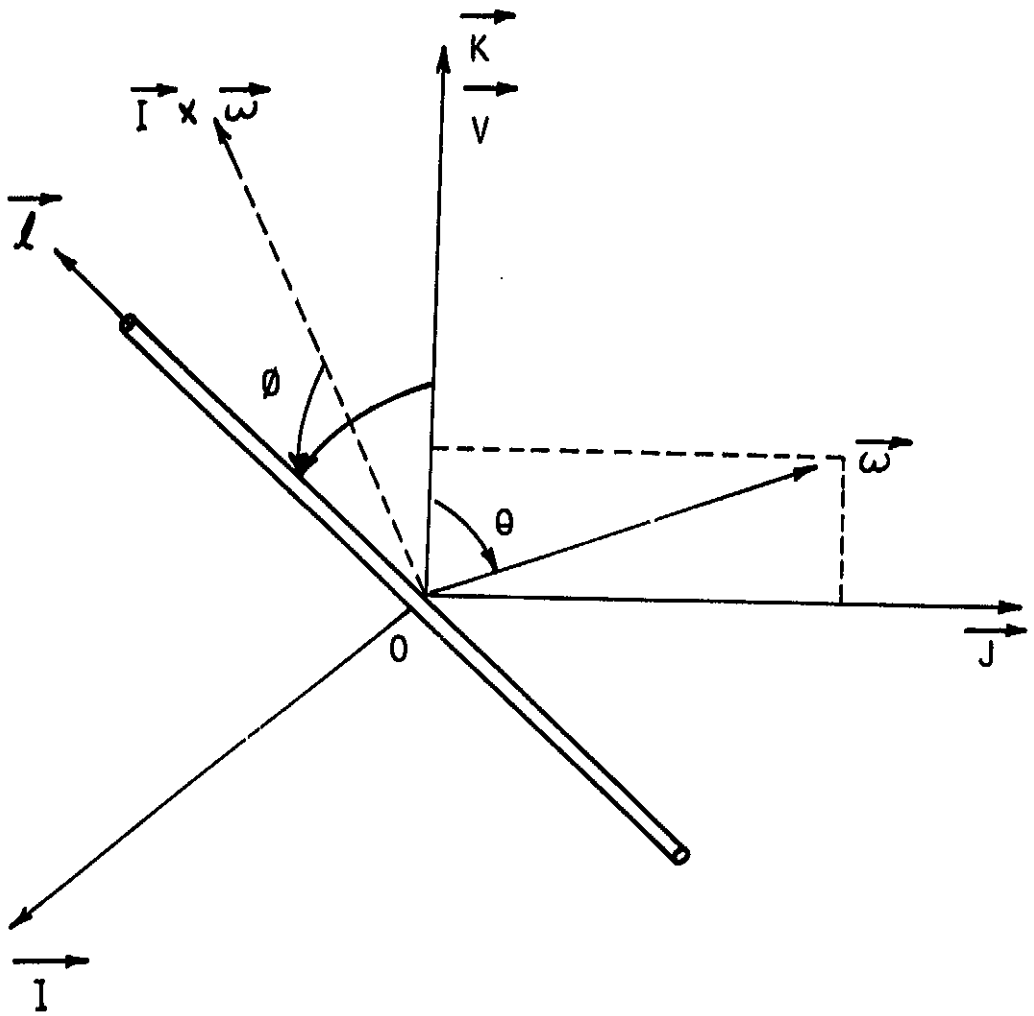

FIGURE 2 - COORDINATE SYSTEM FOR A TUMBLING CYLINDER

FIGURE 3 - TUMBLING EFFECT AND SHAPE FACTOR IN FREE MOLECULAR FLOWS

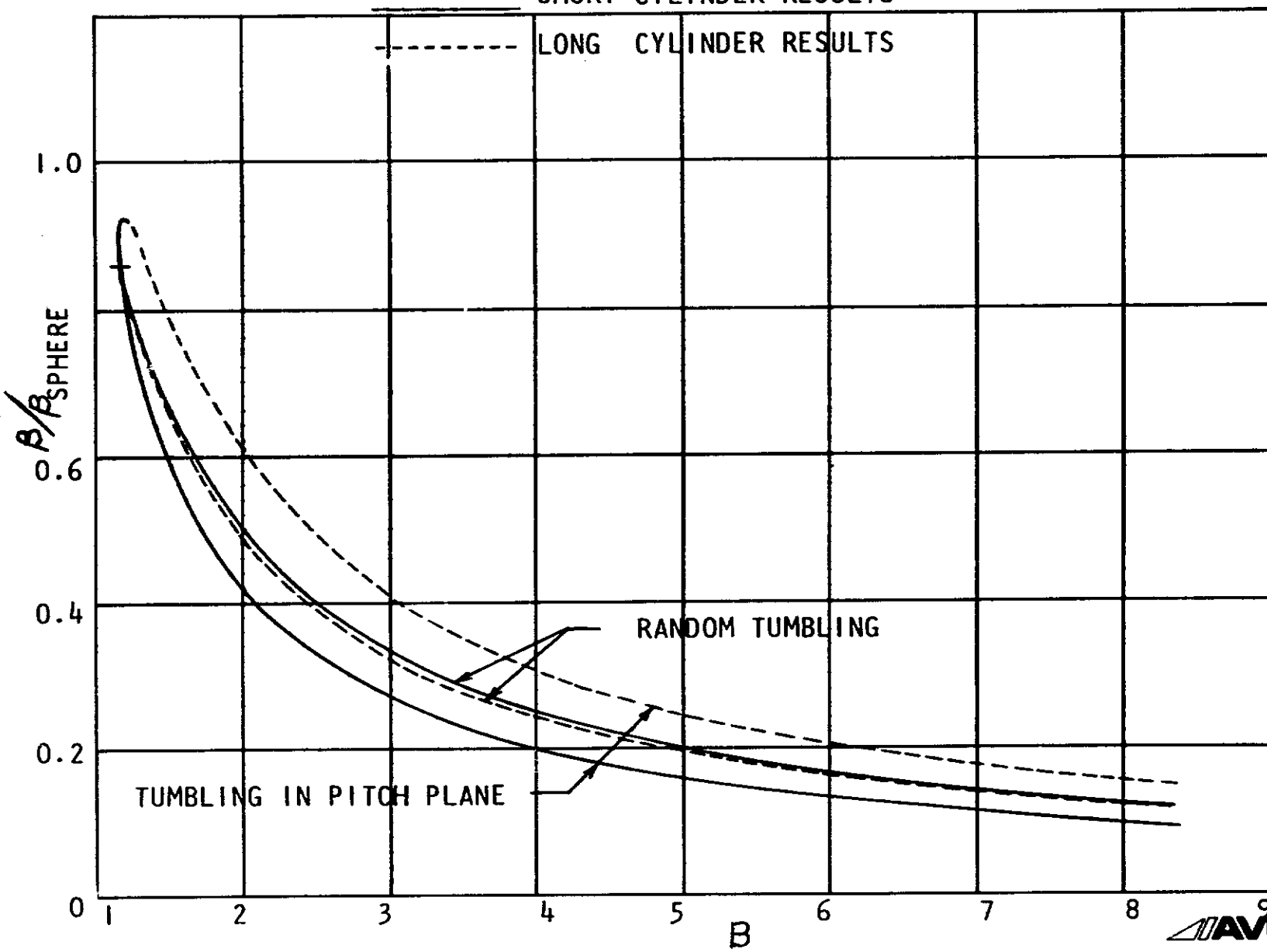

FIGURE 4 - TUMBLING EFFECT AND SHAPE FACTOR IN CONTINUUM FLOWS

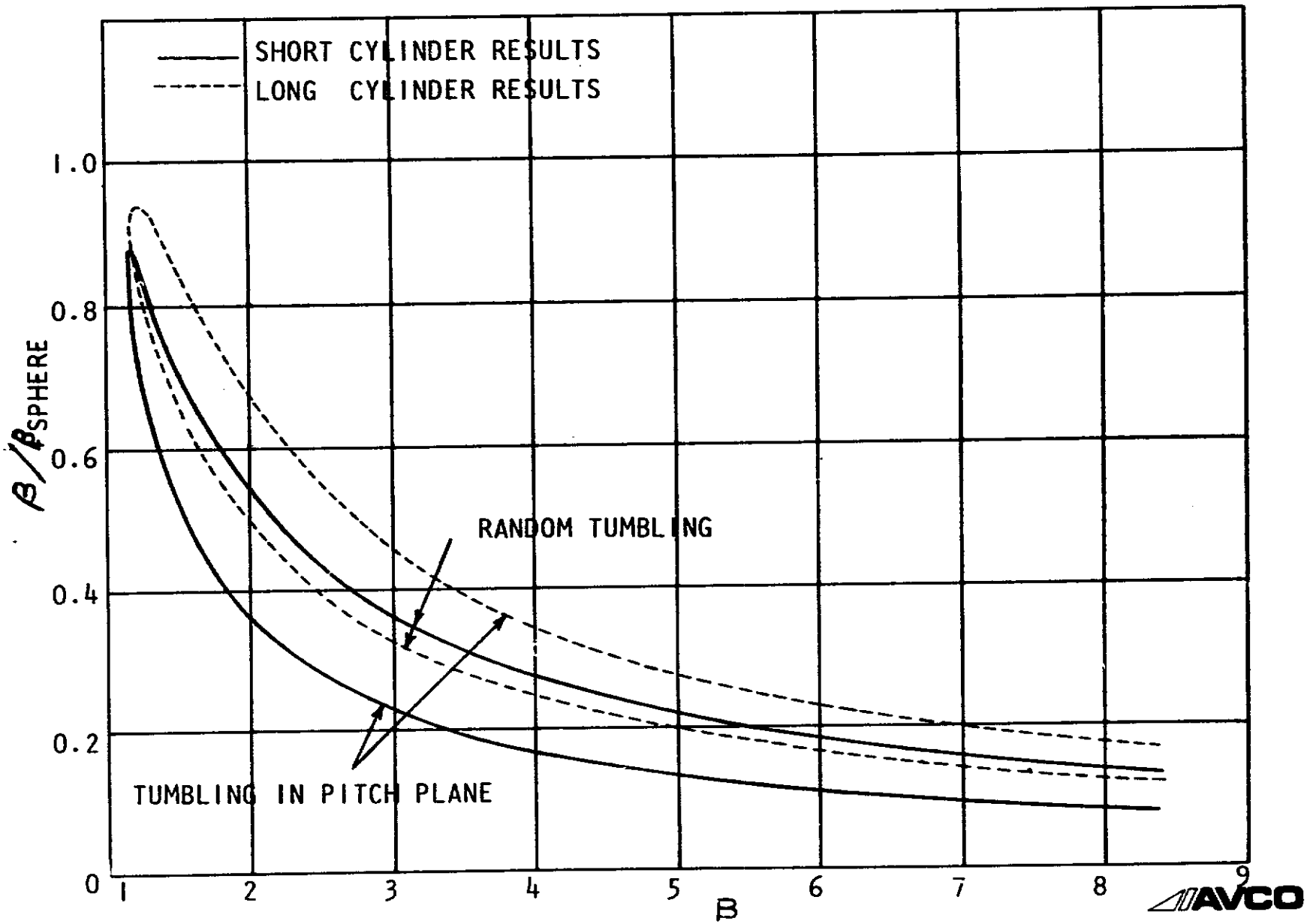

FIGURE 5 - VARIATION OF DRAG COEFFICIENT IN TRANSITION REGION

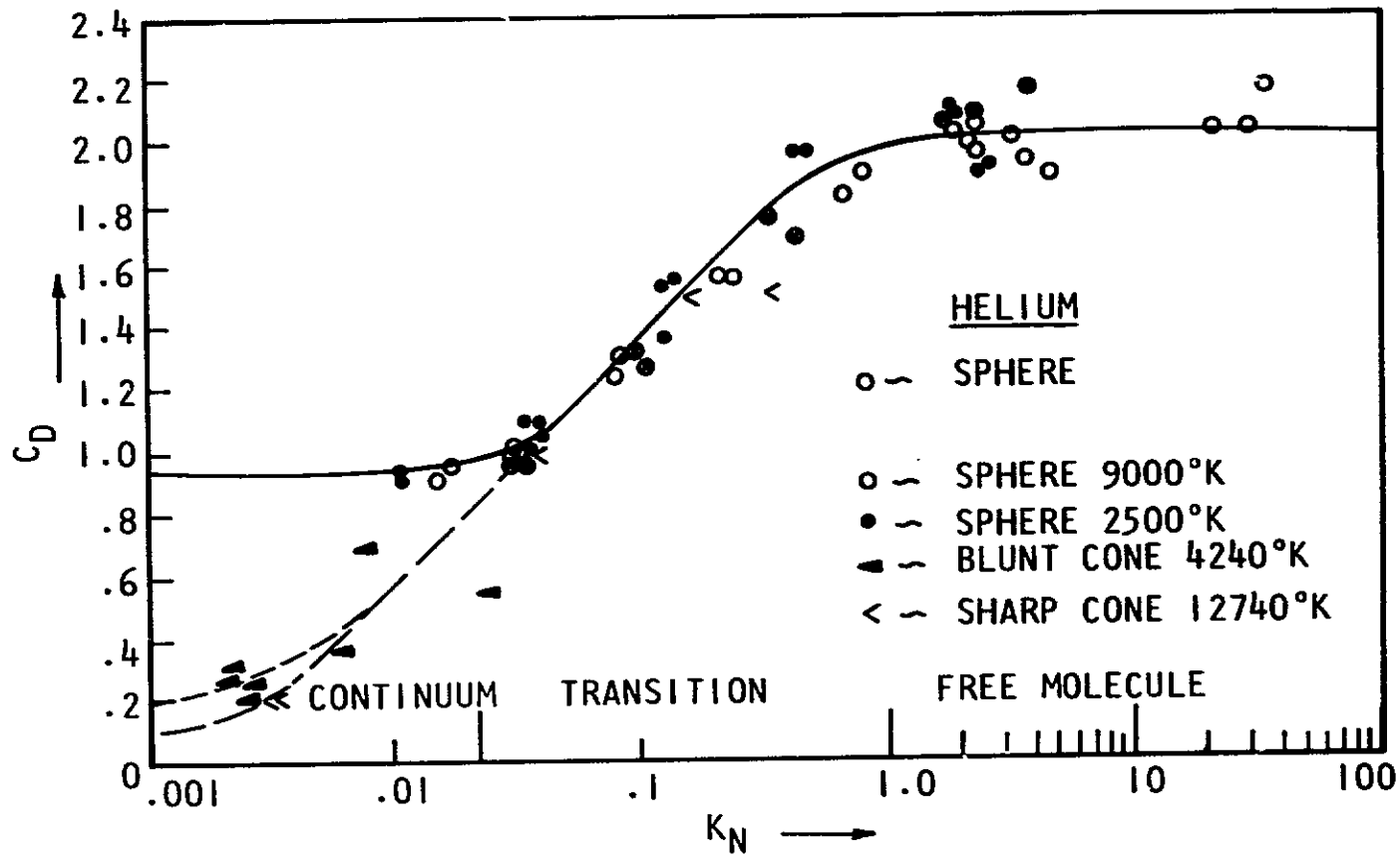

FIGURE 6 - SKIN-FRICTION DRAG COEFFICIENT AS A FUNCTION OF THE "INTERACTION" PARAMETER (FROM REFERENCE 9)

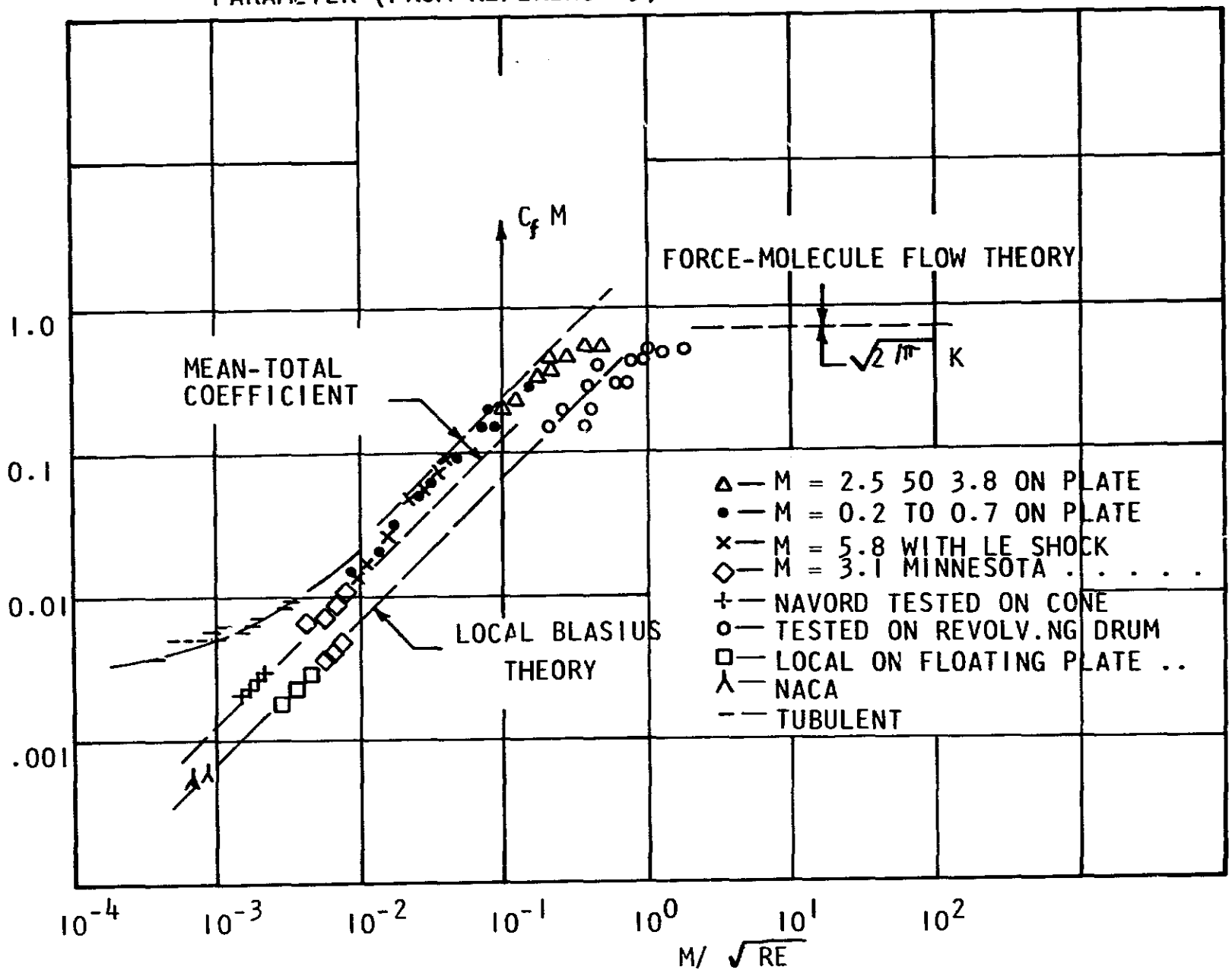

FIGURE 7 - SURFACE ROUGHNESS ON DRAG

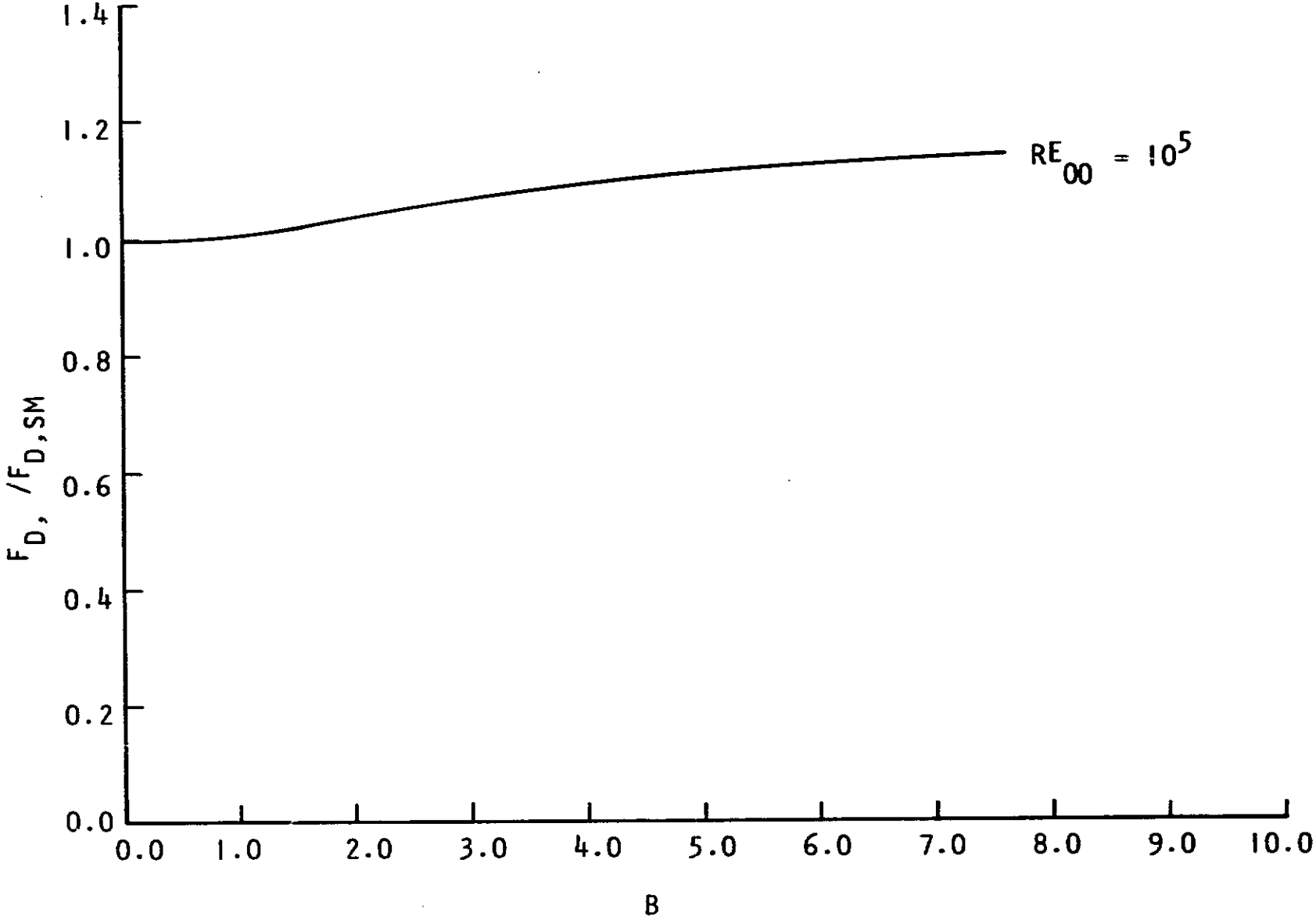

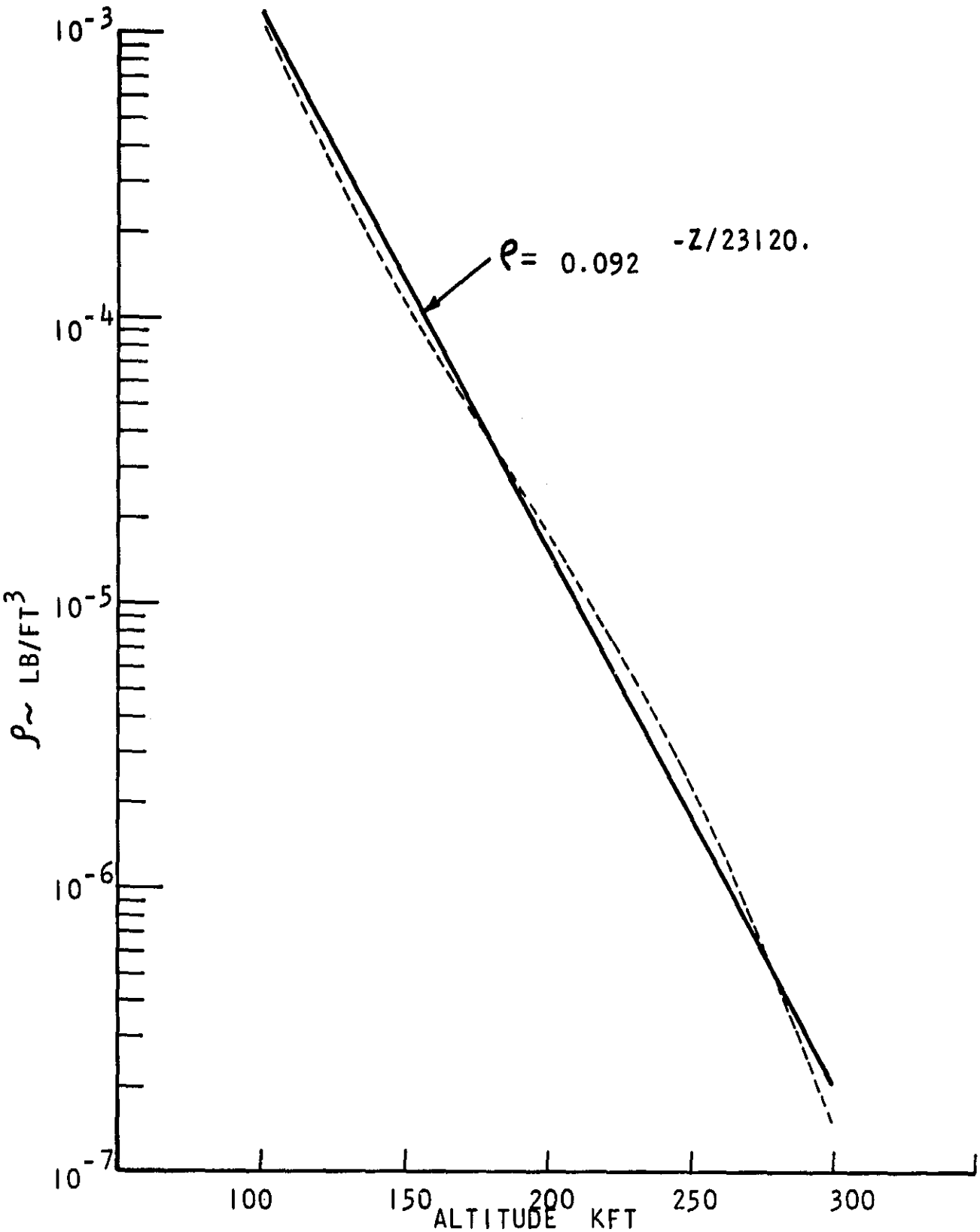

FIGURE 8 - HIGH ALTITUDE AIR DENSITY DISTRIBUTION

FIGURE 9 - TUMBLING EFFECT ON CONSOLIDATING ALTITUDE WITH FREE-MOLECULAR

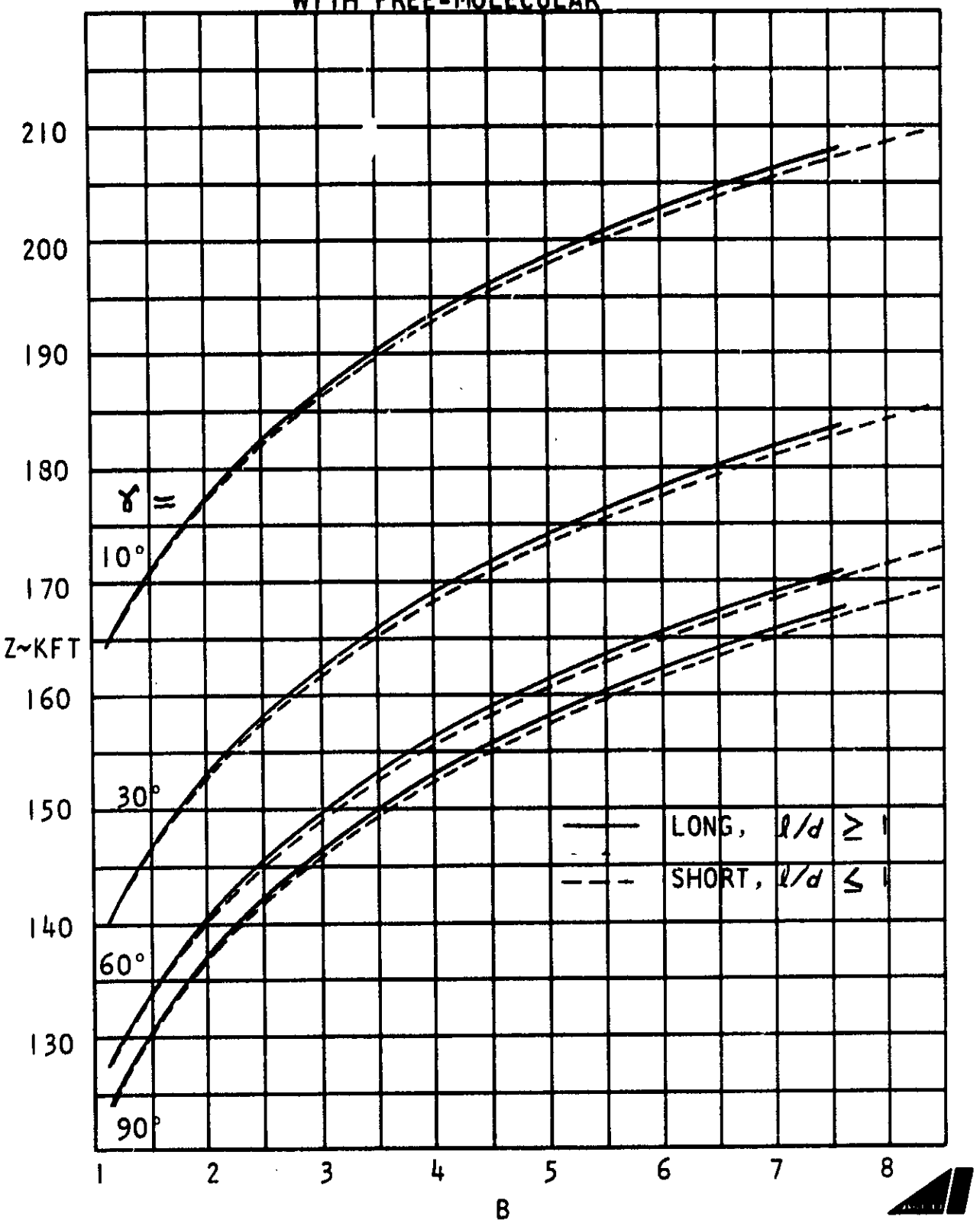

FIGURE 10 - TUMBLING EFFECT ON CONSOLIDATING ALTITUDE WITH CONTINUUM β

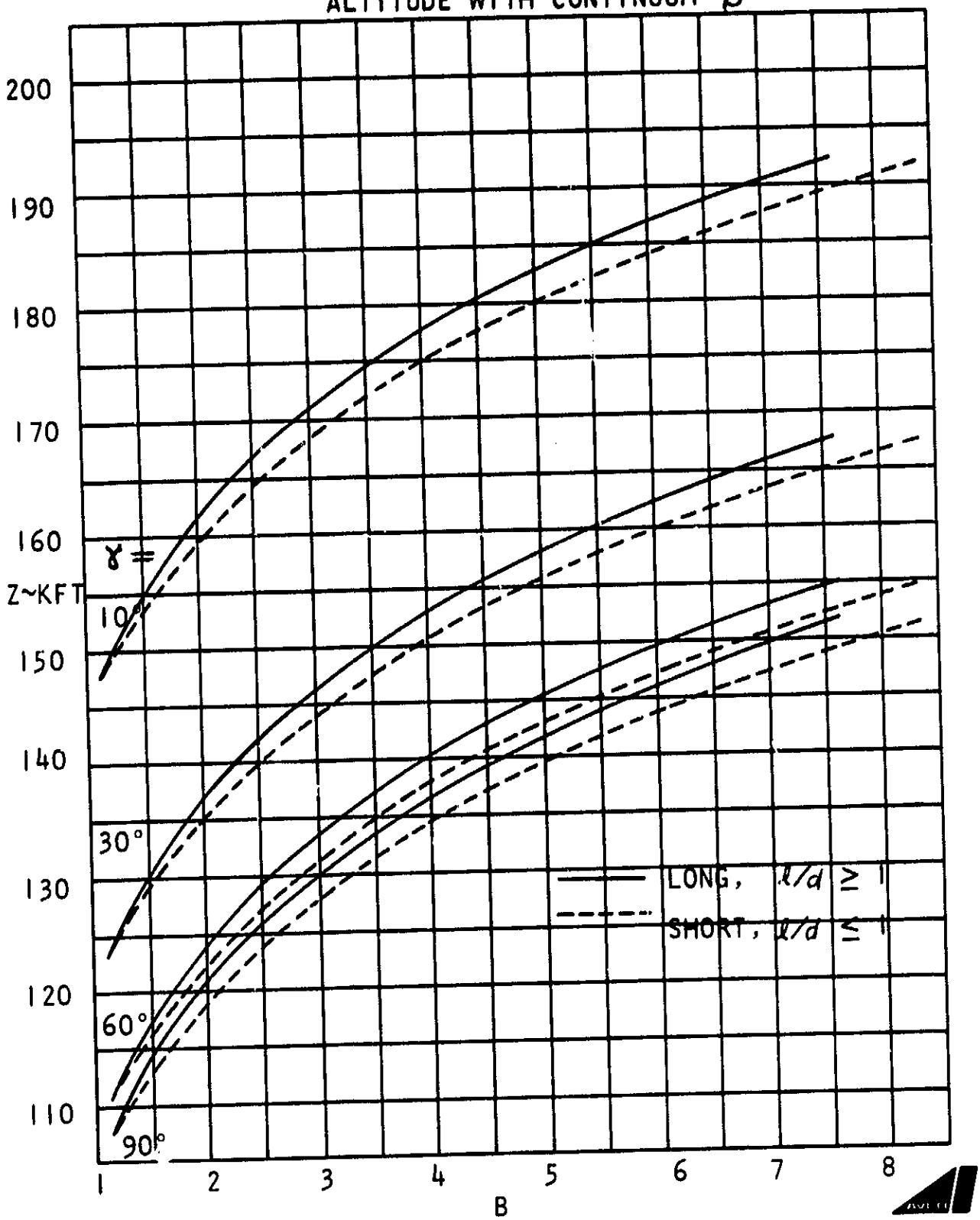

FIGURE 11 - TUMBLING EFFECT ON TOTAL RECESSION (FREE-MOLECULAR)

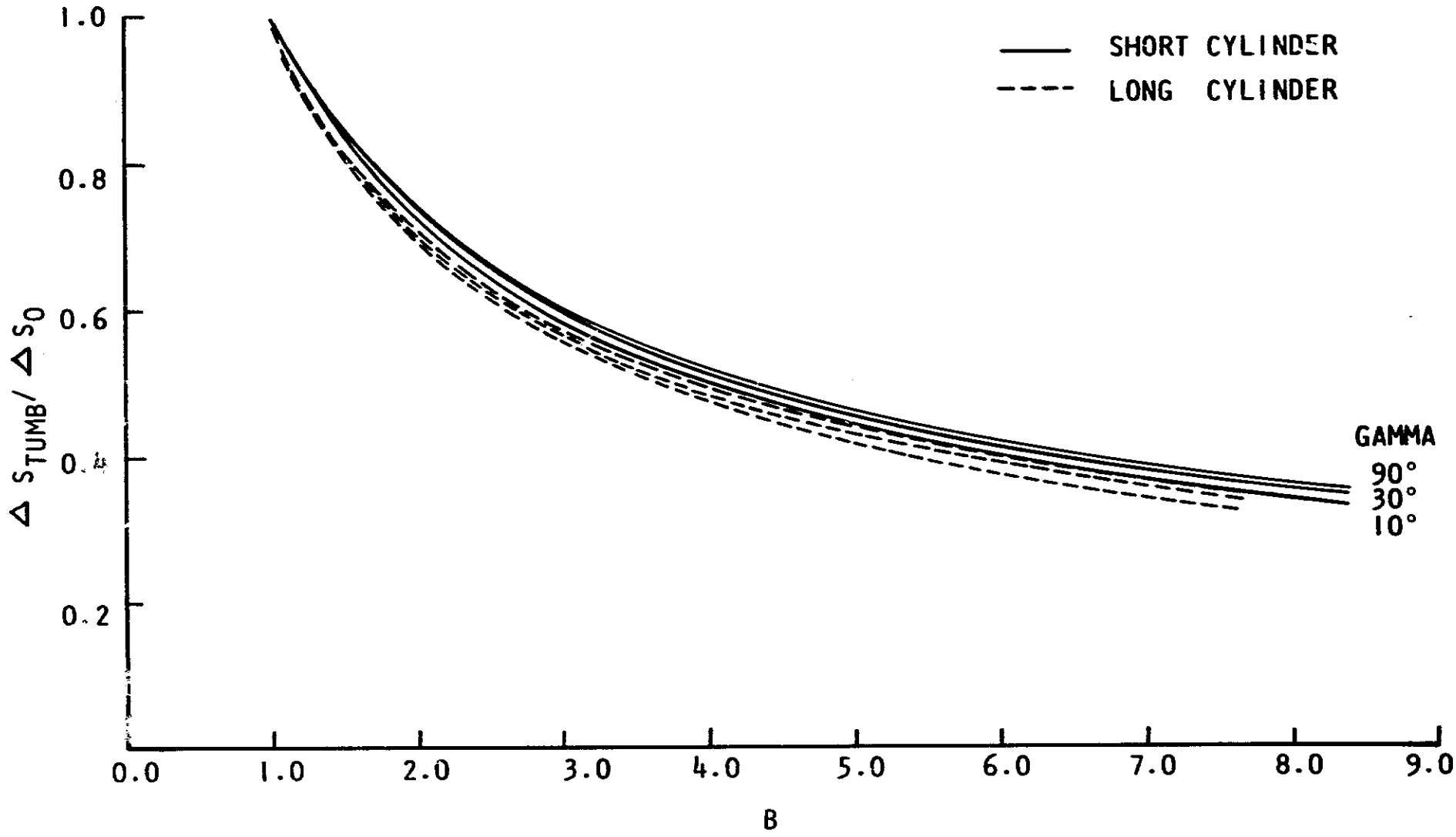

FIGURE 12 - TUMBLING EFFECT ON TOTAL RECESSION (CONTINUUM)